

# A new approach to numerical modelling of temperature fields in metal working processes with experimental verification

Nagib Neimarlija<sup>(1)</sup> and Leopold Škerget<sup>(2)</sup>

<sup>(1)</sup>Faculty of Mechanical Engineering, University of Zenica, Fakultetska 1, 72000 Zenica, BOSNIA AND HERZEGOVINA, e-mail: nagibn@mf.unze.ba

<sup>(2)</sup>Faculty of Mechanical Engineering, University of Maribor, Smetanova 17, SI-Maribor, SLOVENIA  
e-mail: leo@uni-mb.si

## SUMMARY

*The paper presents the results of experimental measurements and numerical calculations of temperature fields in the "die-moving wire" geometry configuration. Experimental measurements were applied for modelling boundary conditions for numerical models and their verification. Boundary element method (BEM) was used in mathematical modelling of basic differential equations and the technique of subdomains was used to combine different temperature fields in the tool and workpiece into a common problem. This statement defines in short the nature of the new approach to numerical modelling of temperature fields in the technological process of metal forming.*

**Key words:** numerical method, boundary element method, heat transfer, technological process of metal forming.

## 1. INTRODUCTION

The phenomena of generation and transfer of heat in the tool and workpiece in technological processes of metal working and machining have attracted scientific attention in the recent years. The major part of the deformation and friction energy in these processes is transformed into heat that increases the temperature, thus having substantial influence on the tool and object of working. High local thermal loads can have the following consequences: intensive wear and formation of craters in the tool, lower quality of the surface finish and worsened tolerances of products. Investigation and knowledge of thermal effects in technological processes of metalworking are essential in the selection of optimal parameters for the course of the process. Thus, known temperature profiles in real engineering applications are very important for selection of optimum parameters in technological process, for defining the level of local thermal loads, which is one of limiting factors for the improved technological process, as well as for quality of products.

Various thermoelectric, pyrometric and photometric methods were applied to measure temperatures in those processes. Simultaneously with experimental measurements, there were attempts to obtain the same results by numerical methods. They were rather successful as confirmed by many scientific works. The approaches known till now, experimental and numerical, for analysing heat fluxes in technological processes of machining and working (i.e. in cutting, forging, rolling, drawing etc.) were such that the tool and the workpiece were analysed separately [1-3].

This model is based on the Boundary Element Method (BEM) and on the technique of subdomains. It enables a completely new access to these problems, which essentially means that the tool and the workpiece involved in the technological process of metalworking are considered as a unified problem [4]. The process of cold drawing of axially symmetrical steel sections was treated as an example for this experimental and numerical analysis. An important parameter of this technological process is drawing rate, proportional to machine capacity and limited by local thermal loads.

The development of drawing technology is directed towards the development of machine designs with controlled cooling of the tool and workpiece. This may result in: increase of the drawing velocity, reduced tool wear and better quality of products.

## 2. EXPERIMENTAL MEASUREMENTS

Planning of measurements includes the application of suitable instruments, measuring methods and data acquisitions. The optimal selection of the measuring points and drawing parameters was made. An important characteristic of the experiment was its complexity that was reflected in simultaneous measurements of nearly all relevant parameters needed for analysing the drawing process. The following parameters were measured experimentally: the die (tool) temperatures in points A and B, the temperature of the wire surface prior to drawing and during the process, the temperature of the wire surface after drawing and during the process, the

temperature of the cooling water at the entrance into the measuring module, the temperature of the cooling water at the exit from measuring module, the cooling water rate, the ambient temperature, the drawing rate (i.e. wire velocity), the drawing force, the wire diameter prior to and after the drawing, the chemical composition of the wire, the mechanical properties of the wire prior to and after the drawing, the metallographic properties of the wire prior and after the drawing, for more details look in Ref. [4].

The results of experimental measurements were used for:

- Modelling of the boundary conditions in numerical calculations of temperature distribution in the tool (die) and workpiece (wire);
- Verification of calculations of the boundary element method.

Figure 1 presents the detailed drawing with the position of measuring points A and B, while Table 1 shows the results of laboratory measurements. The measurements were made in the laboratory of the Institute for Metals and Technologies in Ljubljana, Slovenia.

Table 1 Results of experimental measurements

Measurement, No.	1	2	3	4	5	6	7	8	9	10	11	12
Cooling water rate, $m^3 \cdot h^{-1}$	0.182278											
Drawing speed, $m \cdot s^{-1}$	0.2833			0.55			0.95			1.583		
Wire cross-section reduction, %	24.3											
Drawing force, kN	2.6	2.5	2.5	2.45	2.5	2.5	2.3	2.4	2.3	2.55	2.66	2.6
Ambient temperature, [ $^{\circ}C$ ]	9.5											
Inlet temperature of cooling water, [ $^{\circ}C$ ]	10.0											
Outlet temperature of cooling water, $^{\circ}C$	11	11	11	11	11	11	11.5	11.5	11.5	12	12	12
Wire surface temperature in front of the die, $^{\circ}C$	9.5											
Wire surface temperature behind the die, $^{\circ}C$	54.5	55	54.5	59	59	58	62	62	63	68	69	68
Temperature in the point A, $^{\circ}C$	37.5	37	37.5	46.5	46	46	70	71	71	82	83	83
Temperature in the point B, $^{\circ}C$	26	26	26	29.5	29	30	40.5	41	41	45	46	45

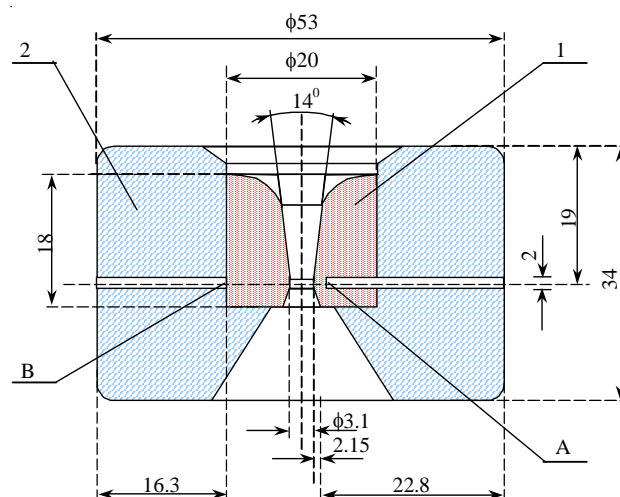


Fig. 1 Die (tool): 1 - core of die (hard metal), 2 - core holder (steel), A and B - measurement points

### 3. BOUNDARY ELEMENT METHOD

#### 3.1 Mathematical model for the temperature field in the tool

##### 3.1.1 Governing equation

The steady energy transport in isotropic and homogeneous body of constant conductivity is described by the following linear elliptic equation for the temperature:

$$\nabla^2 T = 0 \quad \text{in } \Omega \quad (1)$$

where  $T$  is temperature,  $\Omega$  is solution domain and  $\nabla^2$  is Hamilton's nabla operator. The mathematical description of the problem is completed by providing linear boundary conditions: Dirichlet, Neumann and Cauchy.

##### 3.1.2 Boundary integral equation

Differential equation (1) is transformed in boundary integral equation by applying a weighted residual technique or Green's theorem [5]:

$$C(\xi)T(\xi) + \int_{\Gamma} T \frac{\partial T^*}{\partial n} d\Gamma = \int_{\Gamma} \frac{\partial T}{\partial n} T^* d\Gamma \quad (2)$$

where  $C(\xi)$  is geometrical coefficient,  $\Gamma$  is boundary of domain and  $\partial/\partial n$  is partial derivation in the normal direction.

##### 3.1.3 Fundamental solution

Weighted function  $T^*$  in Eq. (2) is the fundamental solution of the homogeneous elliptic equation and it represents the influence of the unit source which acts in the source point  $\xi$  on the reference point  $S$ :

$$T^*(\xi, S) = \frac{1}{2\pi} \ln \frac{1}{r(\xi, S)} \quad (3)$$

where  $\xi$  is source point,  $S$  is field point on boundary and  $r(\xi, S)$  is distance between source and field point.

##### 3.1.4 Discrete form of integral equation

The analytical solution of integral equation (2) is limited to simple examples, without much practical application. Therefore, the solution must be found numerically and the first step is the transformation of Eq. (2) in the discrete form. The discrete matrix form of Eq. (2) can be written as:

$$[H]\{T\} + \frac{\alpha}{\lambda}[G]\{T\} = [G]\{Q\} + \frac{\alpha}{\lambda}[G]\{T_a\} \quad (4)$$

where  $\alpha$  is convection heat transfer coefficient,  $\lambda$  is

heat conductivity coefficient and  $T_a$  is ambient temperature.

The system of algebraic equation (4) for known boundary conditions is transformed in the following system:

$$[A]\{X\} = \{F\} \quad (5)$$

where  $[A]$  is system matrix,  $\{X\}$  is vector of unknowns, and  $\{F\}$  is a known vector.

The system of algebraic equation (5) can be solved with the Gauss elimination method.

#### 3.2 Mathematical model for the temperature field in the workpiece

##### 3.2.1 Governing equation

The steady diffusive-convective energy transport in the isotropic and homogeneous body with constant conductivity and velocity of movement in the  $x$  direction can be described by the following equation for temperature:

$$(V_x \nabla) T = a_0 \nabla^2 T \quad \text{in } \Omega \quad (6)$$

where  $a_0$  is diffusion coefficient,  $V_x$  is velocity in  $x$  direction, that is velocity of the wire, and  $\nabla$  is the Laplace operator.

The mathematical description of the problem is completed by providing linear boundary conditions: Dirichlet, Neumann and Cauchy.

##### 3.2.2 Boundary integral equation

The governing Eq. (6) is transformed in boundary integral equation by applying a weighted residual technique or the Green's theorem for scalar function [6]:

$$C(\xi)T(\xi) + \int_{\Gamma} T \frac{\partial T^*}{\partial n} d\Gamma = \int_{\Gamma} \frac{\partial T}{\partial n} T^* - \frac{1}{a_0} \int_{\Gamma} T T^* V_x n_x d\Gamma \quad (7)$$

##### 3.2.3 Fundamental solution

The weighted function  $T^*$  in Eq. (7) represents the fundamental solution of the equation:

$$a_0 \nabla^2 T - (V_x \nabla) T + \delta(\xi, s) = 0 \quad (8)$$

where  $\delta(\xi, s)$  is the Dirac's delta function and in two-dimensional problems it has the following form [7]:

$$T^* = \frac{1}{2\pi a_0} K_0 \left( \frac{V r}{2 a_0} \right) \exp \left( \frac{V_j r_j}{2 a_0} \right) \quad (9)$$

where  $K_0$  represents the modified Bessel's function of the second kind and zero order.

### 3.2.4 Discrete form of integral equation

Since analytical solution of Eq. (7) is not possible, the problem can be solved only numerically and the first step towards the goal is the transformation of the equation into the discrete form. The discrete form of Eq. (7) can be written as:

$$\begin{aligned}
 [H]\{T\} + \frac{\alpha}{\lambda}[G]\{T\} &= \\
 = [G]\{Q\} + \frac{\alpha}{\lambda}[G]\{T_a\} - \frac{1}{a_0}[G][V_x n_x]\{T\} & \quad (10)
 \end{aligned}$$

which, for known boundary conditions, can be transformed in the following system of algebraic equations:

$$[A]\{X\} = \{F\} \quad (11)$$

The system of algebraic equations (11) can be solved with the Gaussian elimination method.

### 3.3 Subdomain technique

In real engineering problems, the application of the techniques of subdomains is inevitable. It represents the procedure of the division of the basic domain into subdomains, for which the boundary elements method can be applied in the same way as for the basic domain. The mutual position of subdomains can be a contacting one or an overlapping one, which means that different algorithms for solving the obtained system of algebraic equations are applied. The standard method is using the techniques of contacting subdomains and the obtained system of algebraic equations is suitable for direct solving.

The techniques of subdomains were initially developed for the problems with solids in which single sections or subdomains had different physical properties [8], e.g. different conductivities. In problems with branched or thin geometry, it is essential to divide the domains into a necessary number of subdomains to assure the exactness and efficiency of the numerical procedure. In such a case, the integration of the boundary and the domain integrals is shorter since only points from actual subdomains take part in the calculations. This technique enables that subdomains are linked into a unity in the frame of an approximative method when a greater number of subdomains with different basic equations due to various physical phenomena are used. Thus, they can be analysed as a unified model [9]. The analysis of the techniques of subdomains for two solids in close contact will be made for the case when one solid is moving, e.g. when it is actually moving along one axis, in this paper it is  $x$  axis.

On the edge of contact  $\Gamma_f$ , heat is generated due to friction between  $\Omega_1$  and  $\Omega_2$  subdomains. These two physically different temperature fields have a common

edge  $\Gamma_f$  where a joint temperature field is created due to the techniques of subdomains. On this interface the following conditions are valid:

$$T_f = T_f^D = T_f^{DC} \quad (\text{compatibility}) \quad (12)$$

and:

$$q_f = q_f^D + q_f^{DC} \quad (\text{equilibrium}) \quad (13)$$

where  $q_f$  is total friction heat (in our case between wire and die),  $q_f^D$  is the part of friction heat transported over domain  $\Omega_1$  (i.e. die) and  $q_f^{DC}$  is the part of friction heat transported over domain  $\Omega_2$  (i.e. wire), see Figure 2.

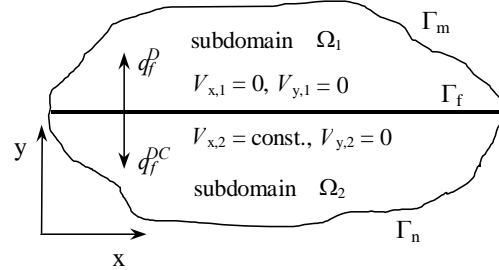


Fig. 2 Definition of the problem

If heat is not generated on the interface boundary, then the equilibrium condition attains the following form:

$$q_f^D = -q_f^{DC} \quad (14)$$

where subscript  $f$  means friction, superscript  $D$  is diffusion and  $DC$  is diffusion-convection.

The  $\Omega_1$  subdomain has  $m+f$  and the  $\Omega_2$  subdomain  $n+f$  boundary elements, and it is supposed that the boundary element method (BEM) is applied in numerical procedure for both subdomains. For the  $\Omega_1$  subdomain the system of algebraic equation  $[A]\{X\} = \{F\}$  obtained by numerical BEM procedure can be (according to Figure 2) separated in the following way:

$$\begin{bmatrix} A_m^D & A_{mf}^D \\ A_{fm}^D & A_f^D \end{bmatrix} \begin{Bmatrix} X_m^D \\ T_f^D \end{Bmatrix} = \begin{Bmatrix} F_m^D \\ q_f^D \end{Bmatrix} \quad (15)$$

The same way on the same level of numerical procedure for the  $\Omega_2$  subdomain gives:

$$\begin{bmatrix} A_f^{DC} & A_{fn}^{DC} \\ A_{nf}^{DC} & A_n^{DC} \end{bmatrix} \begin{Bmatrix} T_f^{DC} \\ X_n^{DC} \end{Bmatrix} = \begin{Bmatrix} q_f^{DC} \\ F_n^{DC} \end{Bmatrix} \quad (16)$$

Combining the equation systems (15) and (16), summing the corresponding algebraic equations and taking into account the conditions (12) and (13) or (14) on the interface, the following joint system is obtained:

$$\begin{bmatrix} A_m^D & A_{mf}^D & 0 \\ A_{fm}^D & (A_f^D + A_f^{DC}) & A_{fn}^{DC} \\ 0 & A_{nf}^{DC} & A_n^{DC} \end{bmatrix} \begin{Bmatrix} X_m^D \\ T_f \\ X_n^{DC} \end{Bmatrix} = \begin{Bmatrix} F_m^D \\ q_f \\ F_n^{DC} \end{Bmatrix} \quad (17)$$

The system of algebraic equations (17) is the known system, as  $[A]\{X\} = \{F\}$ , which can be solved

by the method of the Gaussian elimination. Also, it is important to note that system (17) has  $(m+n+f) \cdot (m+n+f)$  dimension.

#### 4. NUMERICAL CALCULATIONS

The computer program, named Heat2DCS, was developed and used for the calculation of the temperature field in the “die-moving wire” geometry configuration and it has the following advantages: it solves the diffusion-convective heat transport; on the interface it incorporates friction heat generated by the friction of contacting subdomains into calculation; it combines two physically different temperature fields into a unified system by the techniques of subdomains, e.g. diffusion and diffusion-convective one in this case.

The mentioned advantages of the Heat2DCS programme enable a complete computer simulation of heat fluxes and temperature fields in the tool and workpiece in the technological processes of metalworking. The abbreviation Heat2DCS stands for: heat, two dimensions, diffusion, convection and steady state. For the temperature levels created during the experimental measurements, the physical properties of materials shown in Tables 2 and 3 can be taken as constants.

Table 2 Hard metal, subdomains 2 and 3 in Figure 3

Thermal conductivity $\lambda_{hm}, W/m \cdot K$	Specific heat $c_{p,hm}, J/kg \cdot K$	Density $\rho_{hm}, kg/m^3$	Diffusivity $a_{0,hm}, mm^2/s$
73.0	452.0	14300	11.294

Table 3 Wire, subdomain 1 in Figure 3

Thermal conductivity $\lambda_w, W/m \cdot K$	Specific heat $c_{p,w}, J/kg \cdot K$	Density $\rho_w, kg/m^3$	Diffusivity $a_{0,w}, mm^2/s$
59.59	418.7	7760	18.37

A detailed description, type and position of boundary conditions for the geometrical configuration, used in calculations, are presented in Figure 3. The domain of geometric configuration in calculation is composed of the moving wire and the die body. Boundary conditions on AB and KE lines represent joint heat of surface friction between the wire and the die. The second condition is the compatibility, and it is the result of calculation. On edges BC and DE, the boundary conditions are given by the ambient temperature  $T_a$ , measured experimentally, and the convection heat transfer coefficient  $\alpha_a$ , which includes forced convection and radiation of the wire into surroundings. The conditions on EFG, IJK and CD edges are given by the ambient temperature  $T_a$  and by the convection heat-transfer coefficient to the surroundings,  $\alpha_a$ . On the GI section of the edge the conditions are given by the average temperature of cooling water  $T_w$  measured experimentally and by the heat-transfer coefficient  $k$ , given by expression:

$$k = \frac{l}{\frac{l}{\alpha_w} + \frac{\delta}{\lambda_{steel}}} \quad (18)$$

where  $\alpha_w$  is convection heat transfer coefficient from the die to the cooling water,  $\delta$  is thickness of the core die holder wall and  $\lambda_{steel}$  is thermal conductivity of the holder wall material (steel).

Temperature fields are the result of modelling and solving the systems of differential equations, i.e. the diffusion and diffusion-convective equations. The temperature profiles for the “die-moving wire” geometry configuration are presented from Figure 4 to Figure 7, where the parameters of the technological process for which the calculation was made and the modelled boundary conditions, respectively, are discussed in details.

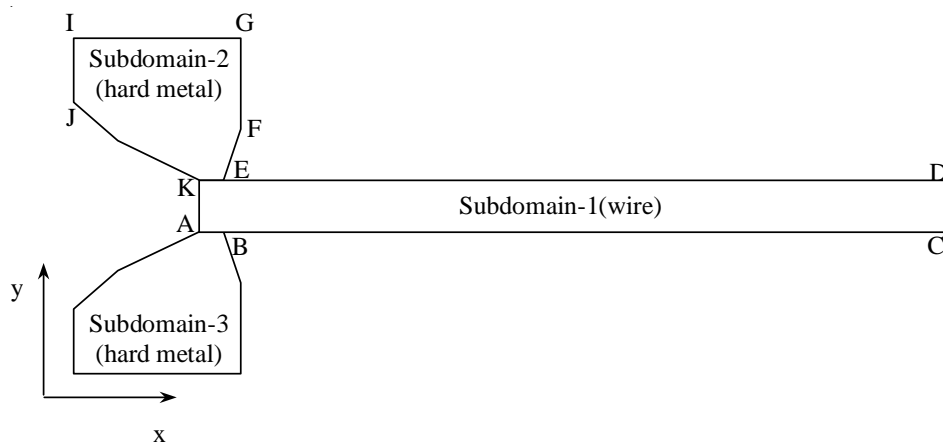


Fig. 3 Definition of the geometry and boundary conditions for the calculated “die-moving wire” geometry configuration, where AB and KE present Neumann’s boundary condition  $\{q_{\beta}\}$ ; BC - Cauchy’s boundary condition  $\{T_a=9.5^{\circ}C, \alpha_a=100 W/m^2 \cdot K\}$ ; CD - Cauchy’s boundary condition  $\{T_a=9.5^{\circ}C, \alpha_a=4.8 W/m^2 \cdot K\}$ ; DE - Cauchy’s boundary condition  $\{T_a=9.5^{\circ}C, \alpha_a=100 W/m^2 \cdot K\}$ ; EFG - Cauchy’s boundary condition  $\{T_a=9.5^{\circ}C, \alpha_a=4.8 W/m^2 \cdot K\}$ ; GI - Cauchy’s boundary condition  $\{T_w=9.5^{\circ}C, k=2160 W/m^2 \cdot K\}$ ; IJK -  $\{T_a=9.5^{\circ}C, \alpha_a=4.8 W/m^2 \cdot K\}$ ; KA - Dirichlet’s boundary condition  $\{T_D=55^{\circ}C\}$

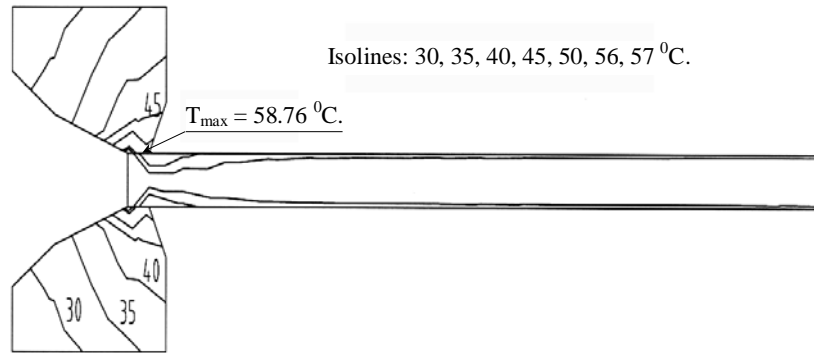


Fig. 4 Temperature profile in the “die-moving wire” geometry configuration for the following conditions of drawing: low-carbon wire with 0.1% C; wire diameter  $D=3.1$  mm; cross section reduction  $R=24.3\%$ ; dry lubrication; drawing velocity  $V_{x,1}=0.2833$  m/s; friction coefficient  $\mu=0.062$ ; convection heat transfer coefficient between the die and the environment  $\alpha_a=4.8$  W/m<sup>2</sup>·K; convection heat transfer coefficient between the wire and the environment  $\alpha_w=100$  W/m<sup>2</sup>·K (which includes convection and radiation); convection heat transfer coefficient on cooling water  $\alpha_w=5400$  W/m<sup>2</sup>·K; thermal conductivity of steel, i.e holder of hard metal  $\lambda_{steel}=59.59$  W/m·K; thermal conductivity of hard metal  $\lambda_{hm}=73$  W/m·K; average temperature of cooling water  $T_w=10.5$ °C; temperature of the deformed wire  $T_D=55$ °C

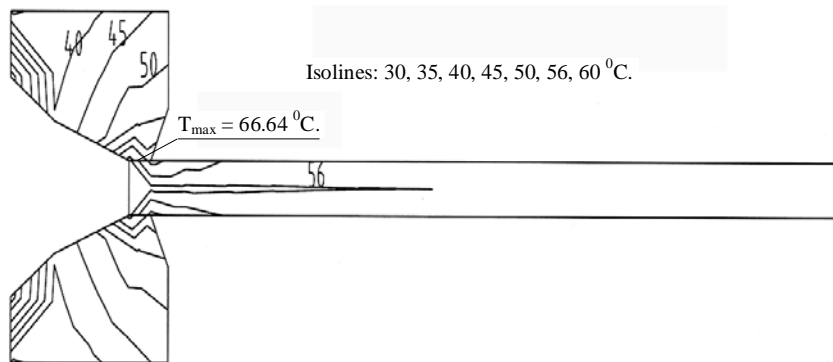


Fig. 5 Temperature profile in the “die-moving wire” geometry configuration for the following conditions of drawing: low-carbon wire with 0.1% C; wire diameter  $D=3.1$  mm; cross section reduction  $R=24.3\%$ ; dry lubrication; drawing velocity  $V_{x,2}=0.55$  m/s; friction coefficient  $\mu=0.062$ ; convection heat transfer coefficient between the die and the environment  $\alpha_a=4.8$  W/m<sup>2</sup>·K; convection heat transfer coefficient between the wire and the environment  $\alpha_w=100$  W/m<sup>2</sup>·K (which includes convection and radiation); convection heat transfer coefficient on cooling water  $\alpha_w=5400$  W/m<sup>2</sup>·K; thermal conductivity of steel, i.e holder of hard metal  $\lambda_{steel}=59.59$  W/m<sup>2</sup>·K; thermal conductivity of hard metal  $\lambda_{hm}=73$  W/m<sup>2</sup>·K; average temperature of cooling water  $T_w=10.5$ °C; temperature of the deformed wire  $T_D=55$ °C

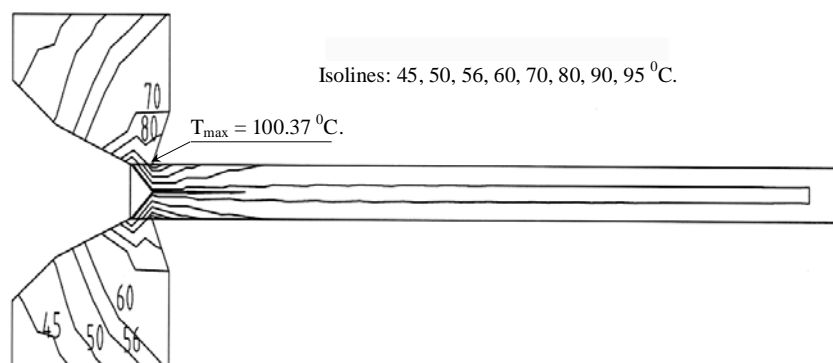


Fig. 6 Temperature profile in the “die-moving wire” geometry configuration for the following conditions of drawing: low-carbon wire with 0.1% C; wire diameter  $D=3.1$  mm; cross section reduction  $R=24.3\%$ ; dry lubrication; drawing velocity  $V_{x,3}=0.95$  m/s; friction coefficient  $\mu=0.048$ ; convection heat transfer coefficient between the die and the environment  $\alpha_a=4.8$  W/m<sup>2</sup>·K; convection heat transfer coefficient between the wire and the environment  $\alpha_w=100$  W/m<sup>2</sup>·K (which includes convection and radiation); convection heat transfer coefficient on cooling water  $\alpha_w=5400$  W/m<sup>2</sup>·K; thermal conductivity of steel, i.e holder of hard metal  $\lambda_{steel}=59.59$  W/m<sup>2</sup>·K; thermal conductivity of hard metal  $\lambda_{hm}=73$  W/m<sup>2</sup>·K; average temperature of cooling water  $T_w=10.5$ °C; temperature of the deformed wire  $T_D=55$ °C

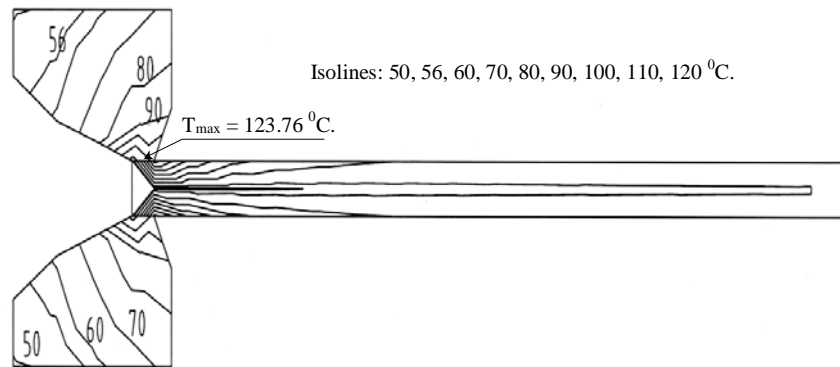


Fig. 7 Temperature profile in the “die-moving wire” geometry configuration for the following conditions of drawing: low-carbon wire with 0.1% C; wire diameter  $D=3.1$  mm; cross section reduction  $R=24.3\%$ ; dry lubrication; drawing velocity  $V_{x,4}=1.583$  m/s; friction coefficient  $\mu=0.071$ ; convection heat transfer coefficient between the die and the environment  $\alpha_a=4.8$  W/m<sup>2</sup>·K; convection heat transfer coefficient between the wire and the environment  $\alpha_a=100$  W/m<sup>2</sup>·K (which includes convection and radiation); convection heat transfer coefficient on cooling water  $\alpha_w=5400$  W/m<sup>2</sup>·K; thermal conductivity of steel, i.e holder of hard metal  $\lambda_{steel}=59.59$  W/m<sup>2</sup>·K; thermal conductivity of hard metal  $\lambda_{hm}=73$  W/m<sup>2</sup>·K; average temperature of cooling water  $T_w=10.5$ °C; temperature of the deformed wire  $T_D=55$ °C

## 5. VERIFICATION OF THE NUMERICAL CALCULATIONS

New numerical models can be tested on simple examples, which have analytical solutions, or with experimental measurements for real calculated geometrical configuration. In our case we have chosen experimental verification of the numerical model. Therefore, Table 4 presents the results of experiments and numerical calculations of temperature in A and B points.

The temperature  $T_{max}$  is the compatibility condition, Eq. (12), which is the result of the numerical calculation and it represents the temperature in the contact between the tool and the workpiece. Unfortunately, it is not possible to determine the temperature  $T_{max}$  experimentally. However, its

numerically calculated value could be accepted as real, if agreement of results between experiment and BEM in the points A and B is satisfactory. It should be highlighted that knowledge of this temperature is very important since it shows the level of local thermal load in the technological working process.

The presented results in Table 4 show a good agreement, which confirms the validity of the numerical model for basic equations and boundary conditions. In addition, results of numerical calculation for  $T_{max}$  in the Table 4, for four different velocities of wire drawing, could be accepted as satisfactory and used in practice.

Of course, it is possible to make a calculation of this very important wire drawing parameter by the presented numerical model. The calculation could be made for all drawing conditions and is particularly important for drawing velocity.

Table 4 Results for different drawing velocities

Temperature, °C	$T_A$	$T_B$	$T_{max}$
<i>Drawing velocity <math>V_{x,1} = 0.2833</math> m/s</i>			
experiment	37.5	26.0	-
The BEM	39.1	29.3	58.74
<i>Drawing velocity <math>V_{x,2} = 0.550</math> m/s</i>			
experiment	46.0	29.5	-
The BEM	49.19	32.6	66.62
<i>Drawing velocity <math>V_{x,3} = 0.950</math> m/s</i>			
experiment	71.0	41.0	-
The BEM	72.47	44.9	100.5
<i>Drawing velocity <math>V_{x,4} = 1.583</math> m/s</i>			
experiment	83.0	45.0	-
The BEM	88.0	53.0	123.0

## 6. CONCLUSION

Experimental measurements fulfilled their basic task, which was the modelling of boundary conditions for numerical models and their verification. Comparison of calculated and experimentally measured results shows a good agreement, which confirms the correctness of the numerical model for governing differential equations and boundary conditions.

The model is very suitable for optimization of existing technological processes: drawing of axially symmetric sections, forging, cutting, rolling etc. For example, it is possible to investigate very important aspects in the technological process of wire drawing such as: reduction of local thermal loads, increase of drawing rate, improvement of product quality, reduction of consumed electric energy and of auxiliary material consumption etc.

The test examples given in Ref. [4] have shown a great stability of solutions for very small and for big Peclet's numbers, which enables analyses and calculations of temperature fields for all real situations that could appear in practice. It is also possible to enter a field that is technologically not possible yet, i.e. some futuristic analyses can be made as well as research on conditions of their real introduction into practice.

## 7. REFERENCES

- [1] Y. Nakamura, T. Fujit and H. Kawakaru, New cooling system for high speed wire drawing, *Wire Journal*, Vol. 9, pp. 59-68, 1976.
- [2] O. Pawelsk and R. Keuper, Investigation of direct cooling in drawing steel wire, *Wire Journal*, Vol. 1, pp. 86-92, 1984.
- [3] N. Neimarlija, Experimental testing and numerical simulation of temperature in dies for dry steel wire drawing, *Wire Journal*, Vol. 1, pp. 74-82, 1988.
- [4] N. Neimarlija, Numerical modelling of unsteady temperature fields in metal working technological processes, Ph.Thesis, University of Ljubljana, 1996. (in Bosnian)
- [5] C.A. Brebbia, *The Boundary Element Method for Engineers*, Pentech Press, London, 1978.
- [6] N. Okamoto, Analysis of convective diffusion problem with first order chemical reaction by BEM, *Int. J. Num. Meth. Eng.*, Vol. 8, pp. 55-64, 1988.
- [7] L.C. Wrobel and D.B. DeFigueiredo, A dual reciprocity boundary element formulation for convection-diffusion problems with variable velocity fields, *Engineering Analysis with Boundary Elements*, Vol. 8, pp. 312-319, 1991.
- [8] R. Bialecki and A. Nowak, Boundary value problems in heat conduction with non linear material and non linear boundary conditions, *Applied Math. Modelling*, Vol. 5, pp. 417-421, 1981.
- [9] I. Žagar, M. Hriberšek, L. Škerget and A. Alujević, A study of flow structures in a cavity due to double-diffusive natural convection by boundary element method and sub-domain technique, Proc. 13<sup>th</sup> Int. Conf. on Boundary Element Methods, Eds. C.A. Brebbia and G.S. Gipson, Computation Mechanics Publications, Southampton, 1991.

## NOVI PRISTUP NUMERIČKOM MODELIRANJU TEMPERATURNIH POLJA U PROCESIMA OBRADJE METALA S EKSPERIMENTALNIM DOKAZIMA

### SAŽETAK

Ovaj rad iznosi rezultate eksperimentalnih mjerenja i numeričkih izračuna temperaturnih polja u "die-moving-wire" geometrijskoj konfiguraciji. Eksperimentalna mjerenja su primjenjivana za modeliranje rubnih uvjeta za numeričke modele kao i njihovu verifikaciju. Metoda rubnih elemenata (BEM) koristila se u matematičkom modeliranju osnovnih diferencijalnih jednadžbi, a tehnika područja poddomena koristila se da bi se sjedinila različita temperaturna polja u alatu i predmetu obrade u zajednički problem. Navedeno ukratko definira prirodu novog pristupa u numeričkom modeliranju temperaturnih polja u tehnološkim procesima oblikovanja metala.

**Ključne riječi:** numerička metoda, metoda rubnih elemenata, prijenos topline, tehnološki proces oblikovanja metala.